(Received 17 October 2025, Accepted 1 December 2025, Scheduled 12 December 2025)

Single-Fed Dielectric Resonator Antenna with Large Frequency Ratio Based on Metasurface

Wenhan Wan[1,2], Wusheng Ji[1,2,*], Zhaoyi Wang[1,2], and Xingyong Jiang[3]

[1]School of Electronic Engineering, Tianjin University of Technology and Education, Tianjin 300222, China
[2]Institute of Antenna and Microwave Techniques, Tianjin University of Technology and Education, Tianjin 300222, China
[3]Rofs Microsystem, Tianjin 300462, China

ABSTRACT: This paper proposes a single-fed antenna with large frequency ratio. The antenna integrates a metasurface antenna and a dielectric resonator antenna (DRA), capable of simultaneous operation in both microwave and millimeter-wave bands with single-port feeding. The microwave band achieves resonance through the metasurface antenna, while the millimeter-wave band resonates by exciting the $HEM_{12\delta}$ higher-order mode of the DRA. The proposed metasurface antenna achieves 24% (5.6 GHz–7.13 GHz) impedance bandwidth, 10% (6.2 GHz–6.9 GHz) axial ratio bandwidth, and 6.07 dBi peak gain in the microwave band; the DRA provides 13.4% (27.47 GHz–31.43 GHz) impedance bandwidth and 6.4 dBi peak gain in the millimeter-wave band. With simple structure and excellent performance, this antenna achieves a frequency ratio of 5.2, making it suitable for 5G communication scenarios requiring concurrent Sub-8 GHz and FR2 operation.

1. INTRODUCTION

With the rapid development of wireless communication technologies, microwave band spectrum has become increasingly congested. Millimeter-wave band possesses abundant spectrum resources and higher operating frequencies, enabling greater system capacity and faster data transmission rates, thus attracting significant attention. However, millimeter-wave electromagnetic waves also have limitations, including restricted transmission distance and substantial propagation loss. Consequently, co-existing technology for microwave and millimeter-wave bands has become a crucial research topic in modern wireless communication systems [1, 2]. The most straightforward approach to enable a single antenna to operate in both microwave and millimeter-wave bands is to integrate two separate antennas designed for each respective band [3–5].

Over the past two decades, Dielectric Resonator Antenna (DRA) has garnered significant attention due to its notable advantages, such as small size, low loss, high efficiency, and ease of excitation [6–8]. These advantages enable DRA to be easily integrated with other antennas to achieve dual-band characteristics. For instance, in [9], a DRA designed for resonance in the microwave band (2.4 GHz) was developed, and a conductive slot was embedded to form a Fabry-Perot Resonator Antenna (FPRA) suitable for the millimeter-wave band (24 GHz). This antenna is excited by two different ports for the microwave and millimeter-wave bands. In another design [10], a hollow DRA with an attached FPRA was proposed for dual-band resonance. By employing a dual-port feeding method and precisely positioning the air gap between the FPRA and the hollow region of the DRA, dual-band resonance at 2.4 GHz and 24 GHz was achieved. The DRA was excited using a microstrip line feed, while the FPRA was fed using a WR-34 waveguide. Recently, [11] proposed a multi-port integrated DRA with a large frequency ratio, incorporating MIMO and array configurations. The MIMO antenna achieves resonance in the Sub-6 GHz band through two dielectric elements and in the millimeter-wave band through four array elements.

The dual-band antennas with large frequency ratios discussed in the aforementioned literature employ dual-port or multi-port excitation methods, which inevitably increase the complexity of antenna design. In contrast, dual-band antennas fed by a single port generally exhibit relatively small frequency ratios [12–15]. In [16], a dual-band slot array antenna was designed using a coplanar waveguide, achieving resonances at 18 GHz and 24 GHz with a frequency ratio of 1.33. In [17], the integration of strip-type, slot-type, and rectangular resonators enabled dual-band operation at 28 GHz and 39 GHz (frequency ratio: 1.39). In [18], a partially reflective surface and artificial magnetic conductor were utilized to attain resonances at 2.46 GHz and 5.5 GHz.

Addressing the challenge that single-fed dual-band antennas rarely achieve frequency ratios exceeding 3, this paper proposes a metasurface-based single-fed DRA with large frequency ratio. Utilizing slot-coupled feeding, the antenna achieves dual-band resonance at 5.9 GHz and 30.7 GHz with a frequency ratio of 5.2, while exhibiting broad impedance bandwidth and axial ratio bandwidth in the microwave band. The antenna features a simple structure and superior performance.

* Corresponding author: Wu-Sheng Ji (jiwusheng@tute.edu.cn).

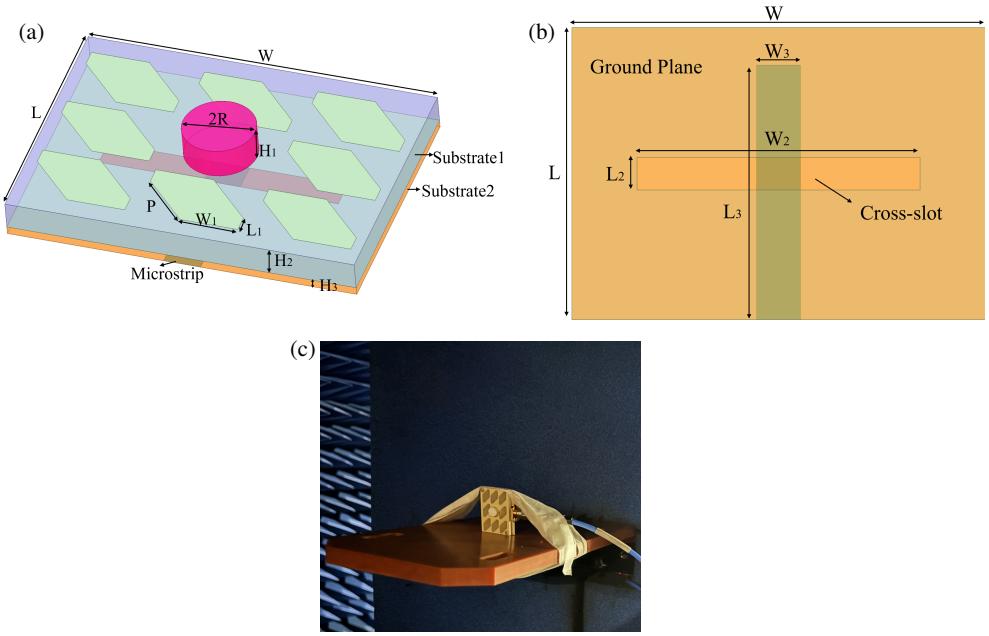

FIGURE 1. Configuration of the proposed antenna. (a) 3D view. (b) Top view of slot. (c) The antenna prototype.

2. ANTENNA DESIGN AND ANALYSIS

2.1. Antenna Structure

The dielectric resonator antenna (DRA) proposed in this paper is illustrated in Fig. 1. It consists of a cylindrical dielectric resonator at the top, a metasurface structure, and a feeding substrate at the bottom. The cylindrical DRA and the metasurface structure at the top are placed on a Rogers 4003 dielectric substrate with a thickness H_2, length L, width W, dielectric constant of 3.38, and loss tangent of 0.0027. The cylindrical DRA structure at the top is made of JJD07-1 dielectric ceramic material with a dielectric constant (ε_r) of 6.7, a height of H_1, and a radius of R. The metasurface structure comprises 8 rhombic metasurface elements with geometric parameters P, W_1, and L_1. The feeding substrate at the bottom also uses a Rogers 4003 dielectric substrate with a thickness of H_3. The upper surface of the dielectric substrate serves as the ground plane, with a rectangular slot etched at its center. The top view is shown in Fig. 1(b), and the geometric parameters are L_2 and W_2. The feeding microstrip line is attached to the bottom surface of the dielectric substrate, with a length of L_3 and a width of W_3. The antenna was characterized by measuring S-parameters using an Agilent E5071C network analyzer and far-field properties using a Satimo StarLab system, with the measurement setup in an anechoic chamber shown in Fig. 1(c). The specific dimensions of the antenna are listed in Table 1.

TABLE 1. Antenna geometry.

Parameters	L	W	H_1	R	H_2	P	W_1
Value/mm	24	34	3	3.5	3.175	6.2	5.6
Parameters	L_1	H_3	L_2	W_2	L_3	W_3	
Value/mm	1.6	0.8	2.7	23.3	20.9	3.6	

2.2. Metasurface Antenna for Lower Band

In the proposed hybrid antenna configuration, the low-band radiation characteristics are primarily governed by the metasurface structure, while the high-band operation mainly relies on the dielectric resonator antenna (DRA) mechanism.

In recent years, characteristic modes have been employed to investigate the operating mechanisms of metasurface antennas. Given that the operating mode of the proposed antenna in the low-frequency band is primarily generated by the metasurface antenna, a characteristic mode analysis is conducted on the metasurface antenna [19]. In characteristic mode technology, Modal Significance (MS) refers to the inherent radiation characteristics of a structure, with $MS = |1/(1 + j\lambda_n)|$. Firstly, the resonant frequency of the metasurface antenna can be determined by analyzing the MS. Secondly, circularly polarized radiation implies that the antenna generates two orthogonal modes with equal MS and a 90° phase difference in their Characteristic Angles (CAs).

Figure 2 displays the modal significance and characteristic angles of the first four modes of the metasurface structure. It can be observed that J_1 and J_2 dominate at 7.15 GHz, with nearly identical MS magnitudes and a characteristic angle difference of approximately 90°. Thus, at 7.15 GHz, J_1 and J_2 satisfy the necessary conditions for circularly polarized radiation.

Figures 3 and 4 present the impedance bandwidth, gain, and axial ratio (AR) performance of the antenna in the low-frequency band. The proposed antenna achieves an impedance bandwidth of 24% (5.6–7.13 GHz), with a peak gain of 6.07 dBi across the matched bandwidth, and provides a 10% axial ratio bandwidth (6.2–6.9 GHz) with fully usable circular polarization coverage. It is noteworthy that certain discrepancies exist between the measured and simulated results, primarily at-

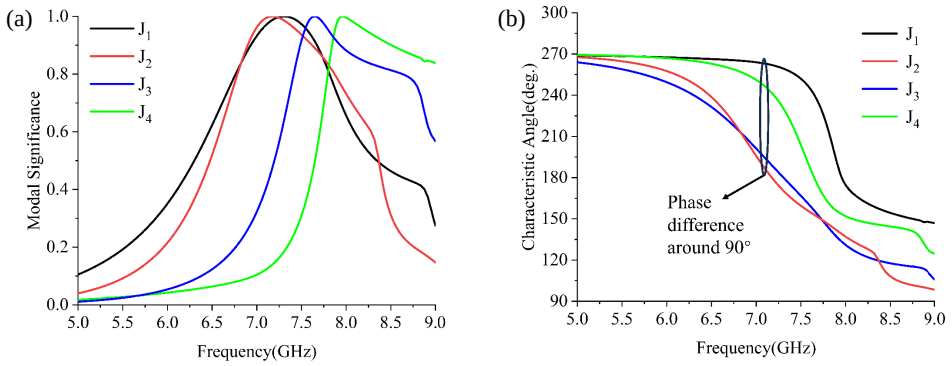

FIGURE 2. MS and CA of the metasurface. (a) MS. (b) CA.

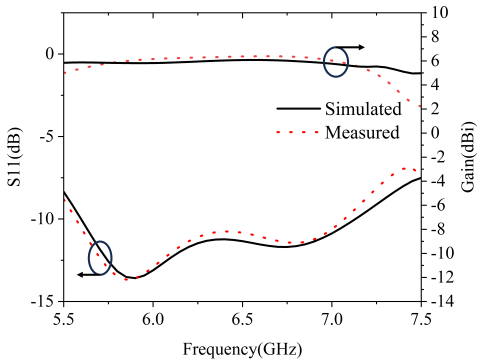

FIGURE 3. Simulated and measured S-parameters and gains.

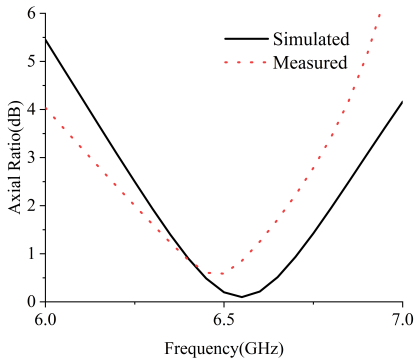

FIGURE 4. Simulated and measured ARs.

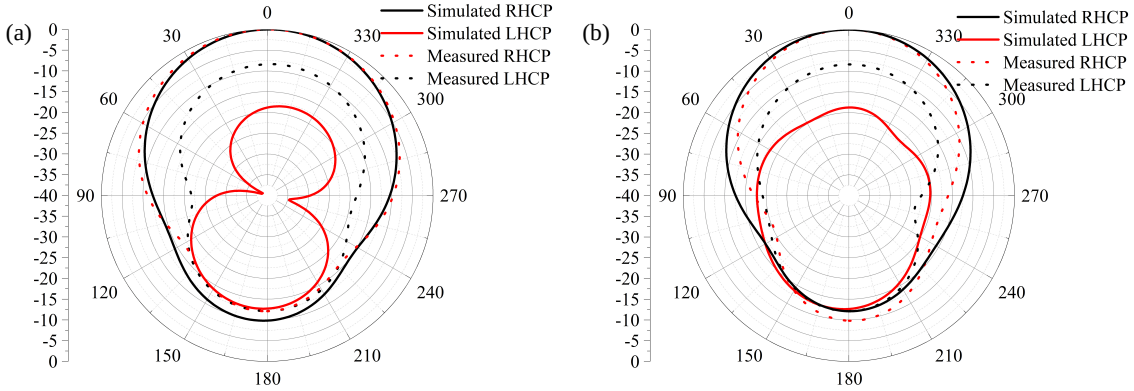

FIGURE 5. Radiation patterns of proposed antenna at 6.55 GHz. (a) $\phi = 0°$. (b) $\phi = 90°$.

tributable to the mechanical fixation method employed for the antenna in this study. Specifically, structural tolerances during mechanical assembly, deformation of dielectric materials under pressure, and minor displacements of connecting components may collectively cause the actual electromagnetic characteristics of the radiating structure to deviate from the ideal simulation model. The mechanical fixation method may also introduce additional parasitic parameters, consequently affecting antenna gain and polarization characteristics.

Figure 5 illustrates the radiation pattern at the minimum axial ratio frequency, specifically at 6.55 GHz. As anticipated, a broadside radiation pattern is achieved in both the $\phi = 0°$ and $\phi = 90°$ planes. In these two planes, the field strength in the right-hand circular polarization (RHCP) direction exceeds that in the left-hand circular polarization (LHCP) direction by more than 20 dBi, indicating that the antenna exhibits right-hand circular polarization.

2.3. DRA for Upper Band

The resonant frequency of a DRA can be initially determined by the Dielectric Waveguide Model (DWM). Assuming that the surface of the DRA is an ideal magnetic conductor, the wave functions for the transverse electric (TE) wave and the transverse magnetic (TM) wave of the DRA are as follows [20]:

$$\psi_{TE_{npm}} = J_n\left(\frac{2X_{np}}{D}\rho\right)\begin{pmatrix}\sin(n\phi)\\ \cos(n\phi)\end{pmatrix}\sin\left[\frac{(2m+1)\pi z}{2H}\right] \quad (1)$$

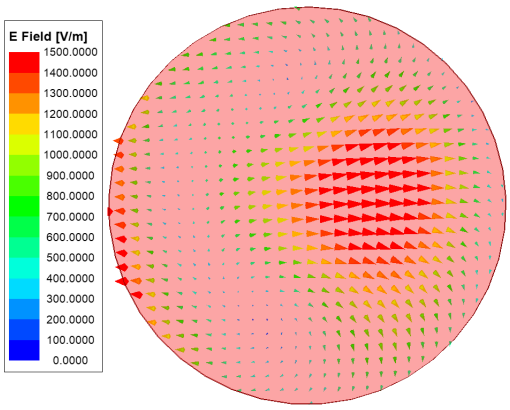

FIGURE 6. Electric field at 28.7 GHz.

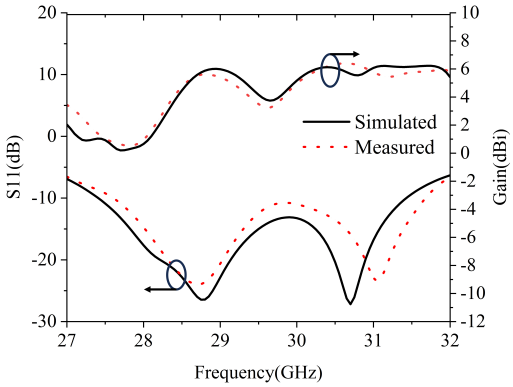

FIGURE 7. Simulated and measured S-parameters and gains.

TABLE 2. Comparison with the related work.

Ref. year.	Ports	f_r (GHz)	Freq. ratio	BW (%)	Gain (dBi)	Size (mm^3)
9 (2019)	2	2.72	9.3	38.2	6.5	$25 \times 24 \times 20$
		25.3		16.2	11.3	
10 (2017)	2	2.73	8.9	30.8	8.23	$48 \times 48 \times 19.4$
		24.4		4.7	17.2	
16 (2024)	1	18	1.3	8.3	14	$15 \times 69.6 \times 4.3$
		24		6.2	17.6	
17 (2023)	1	28	1.4	14.1	6.8	$12 \times 12 \times 1.11$
		39		12.5	6.4	
18 (2022)	1	2.46	2.2	7.2	13.4	$70 \times 70 \times 20.5$
		5.5		16.2	15	
This Work	1	5.9	5.2	24	6.07	$24 \times 34 \times 6.9$
		30.7		13.4	6.4	

$$\psi_{TM_{npm}} = J'_n\left(\frac{2X'_{np}}{D}\rho\right)\begin{pmatrix}\sin(n\phi)\\ \cos(n\phi)\end{pmatrix}\cos\left[\frac{(2m+1)\pi z}{2H}\right] \quad (2)$$

where J_n is the Bessel function of the first kind, with $J_n(X_{np}) = 0$ and $J'_n(X'_{np}) = 0$, $n = 1, 2, 3, \ldots$, $p = 1, 2, 3, \ldots$, $m = 1, 2, 3, \ldots$.

From the separation equation $k_\rho^2 + k_z^2 = k^2 = \omega^2\mu\varepsilon$, the resonant frequency of the $HEM_{12\delta}$ mode in dielectric resonators can be calculated using the following formula:

$$f_{12\delta} = \frac{c}{\pi D\sqrt{\varepsilon}}\sqrt{X_{12}^2 + \left(\frac{\pi D}{4H}\right)^2} \quad (3)$$

where $X_{12} = 5.331$. By using Formula (3), we can obtain a resonant frequency of 29.7 GHz for the cylindrical DRA. Fig. 6 displays the electric field pattern of the DRA at 28.7 GHz. From the electric field distribution shown in Fig. 6, it is confirmed that the $HEM_{12\delta}$ mode is excited at 28.7 GHz. The theoretical analysis results are in good agreement with the numerical analysis results.

Figure 7 shows the antenna's high-band performance, with a 13.4% impedance bandwidth (27.47–31.43 GHz). The gain varies from 0.53 dBi to 6.4 dBi across the band. This fluctuation is an inherent characteristic due to higher-order modes. As shown in Fig. 8, the radiation pattern at 30.7 GHz highlights the outstanding radiation characteristics of the antenna.

Table 2 provides a comparison between the proposed antenna and other dual-band designs. Currently, most antennas capable of operating simultaneously in both microwave and millimeter-wave bands [9, 10] require two separate input ports to support different modes, and the mutual coupling between these ports complicates the design. In contrast, the proposed design achieves a large frequency ratio with only a single-port feed, though it has the drawback of lower gain. Although single-port dual-band antennas have been proposed in the literature [16–18], these antennas struggle to achieve large frequency ratios, thereby limiting their applicability. Furthermore, none of the antennas in the aforementioned studies can simultaneously achieve both a large frequency ratio and circular polarization. In comparison, the proposed antenna achieves a frequency ratio of 5.2, operates in both microwave and millimeter-wave bands with a single feed, and realizes circular polarization in the lower frequency band — all integrated into a compact structure. These characteristics indicate its significant potential for practical applications.

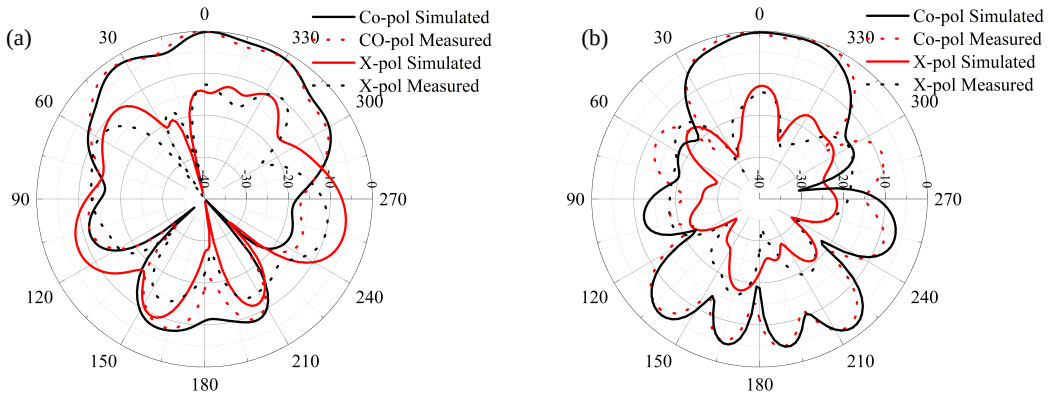

FIGURE 8. Radiation patterns of proposed antenna at 30.7 GHz. (a) $\phi = 0°$. (b) $\phi = 90°$.

3. CONCLUSION

This paper proposes a novel large-frequency-ratio antenna with a single-port feed, which integrates a metasurface antenna and a dielectric resonator antenna. The key feature of this antenna is that it requires only a single-port feed to achieve both a large frequency ratio and circular polarization. Benefiting from its large frequency ratio characteristic, the antenna can simultaneously operate in both microwave and millimeter-wave bands, making it suitable for shared applications in microwave and millimeter-wave scenarios.

ACKNOWLEDGEMENT

This work is supported by Tianjin Key Projects of Research and Development and Science and Technology Support in 2020 (20YFZCGX00700), Tianjin Enterprise Science and Technology Commissioner Project in 2022 (22YDTPJC00330) and 2024 Tianjin Natural Science Foundation (24JCYBJC00860).

REFERENCES

[1] Dehos, C., J. L. González, A. D. Domenico, D. Kténas, and L. Dussopt, "Millimeter-wave access and backhauling: The solution to the exponential data traffic increase in 5G mobile communications systems?" *IEEE Communications Magazine*, Vol. 52, No. 9, 88–95, Sep. 2014.

[2] Choudhury, D., "5G wireless and millimeter wave technology evolution: An overview," in *2015 IEEE MTT-S International Microwave Symposium*, 1–4, Phoenix, AZ, USA, May 2015.

[3] Zhu, X.-Q., Y.-X. Guo, and W. Wu, "Miniaturized dual-band and dual-polarized antenna for MBAN applications," *IEEE Transactions on Antennas and Propagation*, Vol. 64, No. 7, 2805–2814, Jul. 2016.

[4] Lopez, D. G., M. Ignatenko, and D. S. Filipovic, "Low-profile tri-band inverted-F antenna for vehicular applications in HF and VHF bands," *IEEE Transactions on Antennas and Propagation*, Vol. 63, No. 11, 4632–4639, Nov. 2015.

[5] Boukarkar, A., X. Q. Lin, Y. Jiang, and Y. Q. Yu, "Miniaturized single-feed multiband patch antennas," *IEEE Transactions on Antennas and Propagation*, Vol. 65, No. 2, 850–854, Feb. 2017.

[6] Long, S., M. McAllister, and L. Shen, "The resonant cylindrical dielectric cavity antenna," *IEEE Transactions on Antennas and Propagation*, Vol. 31, No. 3, 406–412, May 1983.

[7] Guha, D., A. Banerjee, C. Kumar, and Y. M. M. Antar, "New technique to excite higher-order radiating mode in a cylindrical dielectric resonator antenna," *IEEE Antennas and Wireless Propagation Letters*, Vol. 13, 15–18, 2014.

[8] Luk, K. M. and K. W. Leung, *Dielectric Resonator Antennas*, Research Studies Press, 2003.

[9] Feng, L. Y. and K. W. Leung, "Wideband dual-frequency antenna with large frequency ratio," *IEEE Transactions on Antennas and Propagation*, Vol. 67, No. 3, 1981–1986, Mar. 2019.

[10] Feng, L. Y. and K. W. Leung, "Dual-fed hollow dielectric antenna for dual-frequency operation with large frequency ratio," *IEEE Transactions on Antennas and Propagation*, Vol. 65, No. 6, 3308–3313, Jun. 2017.

[11] Muhammad, A., M. U. Khan, R. S. Malfajani, M. S. Sharawi, and M. Alathbah, "An integrated DRA-based large frequency ratio antenna system consisting of a MM-wave array and a MIMO antenna for 5G applications," *IEEE Open Journal of Antennas and Propagation*, Vol. 5, No. 2, 368–378, Apr. 2024.

[12] Fang, X., K. W. Leung, and E. H. Lim, "Singly-fed dual-band circularly polarized dielectric resonator antenna," *IEEE Antennas and Wireless Propagation Letters*, Vol. 13, 995–998, 2014.

[13] Zhou, Y.-D., Y.-C. Jiao, Z.-B. Weng, and T. Ni, "A novel single-fed wide dual-band circularly polarized dielectric resonator antenna," *IEEE Antennas and Wireless Propagation Letters*, Vol. 15, 930–933, 2015.

[14] Attia, H., A. Abdalrazik, M. S. Sharawi, and A. A. Kishk, "Wideband circularly polarized millimeter-wave DRA array for internet of things," *IEEE Internet of Things Journal*, Vol. 10, No. 11, 9597–9606, Jun. 2023.

[15] Chen, X., J. Wang, and L. Chang, "Extremely low-profile dual-band microstrip patch antenna using electric coupling for 5G mobile terminal applications," *IEEE Transactions on Antennas and Propagation*, Vol. 71, No. 2, 1895–1900, Feb. 2023.

[16] Roy, A., R. Allanic, T. L. Gouguec, F. Gallee, E. Fourn, A.-C. Amiaud, and H. Legay, "A compact dual-band single-feed slotted waveguide array antenna for unidirectional radiation patterns," *IEEE Transactions on Antennas and Propagation*, Vol. 72, No. 12, 9095–9102, Dec. 2024.

[17] Cui, L.-X., X.-H. Ding, W.-W. Yang, L. Guo, L.-H. Zhou, and J.-X. Chen, "Communication compact dual-band hybrid dielectric resonator antenna for 5G millimeter-wave applications," *IEEE Transactions on Antennas and Propagation*, Vol. 71, No. 1, 1005–1010, Jan. 2023.

[18] Qi, J., Q. Wang, F. Deng, Z. Zeng, and J. Qiu, "Low-profile unicavity high-gain FPC antenna covering entire global 2.4 GHz and

5 GHz WiFi-bands using uncorrelated dual-band PRS and phase compensation AMC," *IEEE Transactions on Antennas and Propagation*, Vol. 70, No. 11, 10 187–10 198, Nov. 2022.

[19] Ye, J., T. Li, M. Han, and W. Dou, "Metasurface-inspired wideband circularly polarized antenna array in Ka-band using characteristic mode analysis," *IEEE Antennas and Wireless Propagation Letters*, Vol. 23, No. 1, 389–393, Jan. 2024.

[20] Zhao, G., Y. Zhou, J. R. Wang, and M. S. Tong, "A circularly polarized dielectric resonator antenna based on quasi-self-complementary metasurface," *IEEE Transactions on Antennas and Propagation*, Vol. 70, No. 8, 7147–7151, Aug. 2022.